J Physiol 588.9 (2010) pp 1451–1468

The Journal of Physiology

Regulation of Kv channel expression and neuronal excitability in rat medial nucleus of the trapezoid body maintained in organotypic culture

Huaxia Tong, Joern R. Steinert, Susan W. Robinson, Tatyana Chernova, David J. Read, Douglas L. Oliver and Ian D. Forsythe

The MRC Toxicology Unit, University of Leicester, Leicester LE1 9HN, UK

Principal neurons of the medial nucleus of the trapezoid body (MNTB) express a spectrum of voltage-dependent K^+ conductances mediated by Kv1–Kv4 channels, which shape action potential (AP) firing and regulate intrinsic excitability. Postsynaptic factors influencing expression of Kv channels were explored using organotypic cultures of brainstem prepared from P9–P12 rats and maintained in either low (5 mM, low-K) or high (25 mM, high-K) $[K^+]_o$ medium. Whole cell patch-clamp recordings were made after 7–28 days *in vitro*. MNTB neurons cultured in high-K medium maintained a single AP firing phenotype, while low-K cultures had smaller K^+ currents, enhanced excitability and fired multiple APs. The calyx of Held inputs degenerated within 3 days in culture, having lost their major afferent input; this preparation of calyx-free MNTB neurons allowed the effects of postsynaptic depolarisation to be studied with minimal synaptic activity. The depolarization caused by the high-K aCSF only transiently increased spontaneous AP firing (<2 min) and did not measurably increase synaptic activity. Chronic depolarization in high-K cultures raised basal levels of $[Ca^{2+}]_i$, increased Kv3 currents and shortened AP half-widths. These events relied on raised $[Ca^{2+}]_i$, mediated by influx through voltage-gated calcium channels (VGCCs) and release from intracellular stores, causing an increase in cAMP-response element binding protein (CREB) phosphorylation. Block of VGCCs or of CREB function suppressed Kv3 currents, increased AP duration, and reduced Kv3.3 and c-*fos* expression. Real-time PCR revealed higher Kv3.3 and Kv1.1 mRNA in high-K compared to low-K cultures, although the increased Kv1.1 mRNA was mediated by a CREB-independent mechanism. We conclude that Kv channel expression and hence the intrinsic membrane properties of MNTB neurons are homeostatically regulated by $[Ca^{2+}]_i$-dependent mechanisms and influenced by sustained depolarization of the resting membrane potential.

(Received 24 December 2009; accepted after revision 1 March 2010; first published online 8 March 2010)
Corresponding author I. D. Forsythe: MRC Toxicology Unit, University of Leicester, Leicester LE1 9HN, UK.
Email: idf@le.ac.uk

Abbreviations 2-APB, 2-aminoethoxydiphenylborane; aCSF, artificial cerebrospinal fluid; Aga-IVA, ω-agatoxin-IVA; AP, action potential; CICR, Ca^{2+}-induced Ca^{2+} release; CN, cochlea nucleus; CREB, cAMP-response element binding protein; CTx-GVIA, ω-conotoxin GVIA; DIV, days *in vitro*; DTX, dendrotoxin-I; LSO, lateral superior olive; MNTB, medial nucleus of the trapezoid body; P, post-natal day; Rya, ryanodine; SOC, superior olivary complex; VGCC, voltage-gated calcium channel.

Introduction

A key question of neuronal function is to understand the mechanisms by which the density and activity of voltage-gated ion channels are controlled in native neurons. What forms of homeostatic control enable a neuron to maintain the ideal balance of delayed rectifier to set the phenotypic action potential (AP) firing pattern of any particular neuron? Studies of these processes require an identified neuron in a highly controlled environment. We have chosen the principal neuron of the medial nucleus of the trapezoid body (MNTB) because this neuron has a well characterised response to depolarisation and can be maintained in organotypic tissue culture (Lohmann *et al.* 1998; Lohrke *et al.* 1998).

Well-regulated intrinsic excitability and expression of voltage-gated K^+ channels are vital to balance excitatory drive and to maintain high-fidelity synaptic transmission

© 2010 The Authors. Journal compilation © 2010 The Physiological Society

DOI: 10.1113/jphysiol.2009.186676

in the MNTB (Dodson *et al.* 2002; Schneggenburger & Forsythe, 2006). Several activity-dependent changes in K^+ channels have been observed here: high-frequency auditory stimulation induces rapid dephosphorylation of Kv3.1 channels facilitates high-frequency firing (Song *et al.* 2005); recent evidence demonstrated activity-driven modulation of Kv3 currents by nitrergic signalling (Steinert *et al.* 2008) and reduced Kv1 currents have been observed in the congenitally deaf mouse (*dn*/*dn*) (Leao *et al.* 2004). Studies of acute brain slice preparations are limited to around 8–12 h; however, organotypic slice culture allows chronic changes to be maintained over many days under controlled conditions (Uesaka *et al.* 2005; Baxter & Wyllie, 2006; Gibson *et al.* 2006; Johnson & Buonomano, 2007). The aim of this study was to exploit organotypic brainstem slices to test the effect of depolarization on K^+ channel function and expression in the MNTB.

Studies of activity-dependent mechanisms frequently employ chronically elevated $[K^+]_o$ to generate depolarization-induced neuronal activity (Muller *et al.* 1998; Brosenitsch & Katz, 2001; Zhao *et al.* 2007). In young animals (P3–P5) elevated $[K^+]_o$ was essential for neuron survival in organotypic cultures of the superior olivary complex (SOC) (Lohmann *et al.* 1998; Lohrke *et al.* 1998). Afferent activity is necessary for survival of auditory brainstem neurons at young ages, since cochlea removal in the first postnatal week results in severe cell death in the cochlear nucleus and consequently denervation as well as afferent reorganization in the SOC (Trune, 1982; Russell & Moore, 1995; Tierney *et al.* 1997; Harris & Rubel, 2006). However, little cell loss is found after deafferentation in older animals (Russell & Moore, 1995; Hsieh & Cramer, 2006). This suggests that organotypic brainstem cultures from animals older than P9 may be less sensitive to denervation, permitting examination of other regulatory mechanisms. Synaptic activity contributes to neuronal survival and network development by releasing neurotrophic factors (Rubel & Fritzsch, 2002; Chabbert *et al.* 2003; Tan *et al.* 2008) and regulating synaptic strength and postsynaptic excitability (Desai *et al.* 1999; Nelson *et al.* 2003; Fan *et al.* 2005; Uesaka *et al.* 2005; Xu *et al.* 2005), but in this organotypic culture preparation the major synaptic input to the MNTB does not survive. This creates a model neuronal preparation in which we can study non-synaptic mechanisms of ion channel modulation and may provide insights into mechanisms by which auditory transmission can be maintained when synaptic inputs are compromised, such as following deafness or associated with cochlear implants.

Using MNTB neurons in organotypic cultures from P9–P12 rats, we identify Ca^{2+} and CREB (cAMP-response element binding protein) mediated signalling which modulates K^+ channel expression, consistent with a homeostatic role in tuning neuronal excitability. This regulation is activated by depolarization of the membrane potential and involves voltage-gated calcium channels (VGCCs) and release from intracellular Ca^{2+} stores but without direct involvement of AP firing.

Methods

Preparation of organotypic brainstem slice cultures and acute slices

Nine- to 12-day old Lister–Hooded rats were killed by decapitation in accordance with the UK Animals (Scientific Procedures) Act 1986, and their brains were removed. Organotypic cultures were prepared based on the method of Stoppini *et al.* (1991) with modifications as indicated. The brainstem was dissected in an ice-cold dissecting medium containing: 98% Hanks' balanced salt solution, 1% penicillin–streptomycin (giving 50 units ml^{-1} penicillin and 50 $\mu g\,ml^{-1}$ streptomycin), 25 mM glucose (from 45% glucose solution) and 2 mM kynurenic acid (pH 7.4 when gassed with 95% O_2–5% CO_2). Kynurenic acid is a broad-spectrum antagonist of ionotropic glutamate receptors with preferential affinity for the NMDA receptor (NMDAR; Stone, 1993), and protects neurons from glutamate receptor induced excitotoxicity (Urenjak & Obrenovitch, 2000). Slices for maintenance in culture were prepared under aseptic conditions with sterile solutions.

Brainstem slices were prepared as described previously (Barnes-Davies & Forsythe, 1995). Briefly, the brainstem was mounted in the chamber of a Vibratome (Integraslice 7550, Campden Instruments, Loughborough, UK). Transverse slices (200 μm thick) of the brainstem containing the MNTB were cut in ice-cold dissecting medium. Individual slices were then transferred to 0.4 μm Biopore CM membrane inserts (Millipore, Bedford, MA, USA) placed in six-well culture plates, with each well containing 1.1 ml of culture medium. The low $[K^+]_o$ culture medium contained 5 mM KCl and comprised 97% Neurobasal-A medium (without phenol red), 2% B-27 serum-free supplement, 0.25 mM glutamine solution (Stock: 200 mM, Invitrogen), 0.25 mM Glutamax I solution (Stock: 200 mM, Invitrogen), and 0.1% penicillin–streptomycin solution (Invitrogen) giving 5 units ml^{-1} penicillin and 5 $\mu g\,ml^{-1}$ streptomycin (Kivell *et al.* 2000). The high $[K^+]_o$ culture medium was the same but with addition of 20 mM KCl (added as a solid and filtered). Slices were incubated in a humidified 5% CO_2 atmosphere at 36.5°C. Half of the culture medium was changed twice a week, and the experiments were performed after 7–28 days *in vitro* (DIV). For some experiments, ryanodine (Rya, 100 μM), 2-aminoethoxydiphenylborane (2-APB, 100 μM), KG-501 (12.5 μM) or VGCC inhibitors (nifedipine, 10 μM; ω-conotoxin GVIA, 2 μM; ω-agatoxin

© 2010 The Authors. Journal compilation © 2010 The Physiological Society

IVA, 200 nM) were applied to high $[K^+]_o$ cultured slices and incubated for 24 to 48 h before recording or mRNA extraction. Comparison of neuronal properties was made between treated and control organotypic slices prepared at the same time.

Acute brainstem slices were prepared in the same way as described above, except that instead of dissecting medium, a low-sodium artificial cerebrospinal fluid (aCSF) was used, with a composition of (in mM): 250 sucrose, 2.5 KCl, 10 glucose, 1.25 NaH_2PO_4, 0.5 ascorbic acid, 26 $NaHCO_3$, 4 $MgCl_2$, 0.1 $CaCl_2$, gassed with 95% O_2–5% CO_2 (pH 7.4). Slices were cut and transferred to aCSF containing (in mM): 125 NaCl, 2.5 KCl, 10 glucose, 1.25 NaH_2PO_4, 2 sodium pyruvate, 3 *myo*-inositol, 0.5 ascorbic acid, 26 $NaHCO_3$, 1 $MgCl_2$, 2 $CaCl_2$, gassed with 95% O_2–5% CO_2 (pH 7.4), incubated at 37°C for 1 h and then stored at room temperature until required.

Chemicals were generally obtained from Sigma-Aldrich, UK, but additional substances were obtained from other sources. Invitrogen (UK): penicillin–streptomycin, Neurobasal-A medium without phenol red, B-27 serum-free supplement and Glutamax I. Alomone labs: dendrotoxin-I (DTX-I); Tocris Bioscience (Bristol, UK): Rya and 2-APB. Peptide Institute (Japan): ω-conotoxin GVIA (CTx-GVIA) and ω-agatoxin IVA (Aga-IVA). Contrary to the advertising literature, marked differences were found in neurons cultured with different batches of B-27 serum-free supplement and similar observations have been reported by others (Chen *et al.* 2008). Consequently all experiments in this study were conducted on two batches of B-27 which provided consistent results.

Electrophysiology

For recording, a slice was transferred to a Peltier-controlled environmental chamber on the stage of a Zeiss Axioskop microscope. The chamber was continually perfused (24°C) with gassed aCSF. Individual cells were visualized using differential interference contrast (DIC) optics and a Zeiss Achroplan 63× (0.9) water immersion objective.

Whole-cell patch-clamp recordings were made from principal neurons of the MNTB using an Axopatch 200B amplifier (Molecular Devices, Sunnyvale, CA, USA) or Multiclamp 700B (Molecular Devices). Patch pipettes were pulled by a two stage vertical pipette puller (PC-10, Narishige, Tokyo, Japan) from thick walled borosilicate glass capillaries (GC150F-7.5, Harvard Apparatus Ltd, Edenbridge, UK) to a final resistance of 3–5 MΩ. Patch pipettes were filled with (in mM): 97.5 potassium gluconate, 32.5 KCl, 5 EGTA, 10 Hepes, 1 $MgCl_2$ and 2 NaOH (pH adjusted to 7.2 with KOH and osmolarity adjusted to 295 mosmol l^{-1} with sucrose). For K^+ current measurement, no leak subtraction was performed. A −10.5 mV junction potential (JP) was recorded and *I–V* curves are presented without JP correction.

Whole-cell patch recordings were obtained from MNTB neurons during perfusion of normal aCSF containing 2.5 mM KCl, unless otherwise stated. Voltage-clamp was conducted from a holding potential of −70 mV, and recordings were only made from cells with whole-cell access resistance less than 13 MΩ. Series resistances were compensated >70% with a 10 μs lag time. Voltage-gated currents were evoked by 200 ms voltage steps ranging between −90 mV and +40 mV in 10 mV increments. In current-clamp recordings, the membrane potential of MNTB neurons was adjusted to −70 mV before giving current steps, which ranged from −100 pA to 600 pA in 50 pA increments, to elicit APs.

Signals were amplified and filtered at between 2 and 5 kHz and sampled at between 10 and 20 kHz using an analog-to-digital converter (Digidata 1322a, Molecular Devices). Data were acquired using Clampex 9.2 (Molecular Devices). Current–voltage relations and half-width of action potential durations were analysed using Clampfit 9.2 and Microsoft Excel.

Retrograde Labelling of MNTB neurons

Sterile phosphate-buffered saline (PBS, 0.01 M), pH 7.4, containing 5% dextran tetramethyl-rhodamine of molecular weight 3000 (dextran, D3308, Invitrogen; Oliver *et al.* 2003; Burger *et al.* 2005) was applied using a patch pipette. The pipette was advanced to the lateral superior olive (LSO) region in an organotypic slice viewed using Leica MZ16F fluorescence dissecting microscope. Iontophoretic injections were made using a Constant Current Isolated Stimulator PS3 (Digitimer Ltd, Welwyn Garden City, UK) with a Trigger Generator DG2 (Digitimer) and current of 500 ms 100 μA at 1 Hz lasting 2 min. After 1 h incubation, slices were first examined under fluorescence, and low magnification images were obtained with the Leica dissecting microscope.

Immunohistochemistry

Dextran labelled slices were fixed with 4% paraformaldehyde (PFA) in PBS at 4°C for 30 min and washed thoroughly 3 × 15 min in PBS. Low affinity binding was reduced by overnight incubation (4°C) with buffer containing 10% goat serum and 1% bovine serum albumin (BSA) in PBS with 0.1% Triton X-100 (PBS-T). The primary anti-Kv3.1b antibody (NeuroMab, Davis, CA, USA; 1:1000) was applied in the same buffer for 48 h at 4°C. After washing 3 × 15 min with PBS-T, the slices were incubated with the secondary antibody (goat anti-mouse Alexa-fluor 488, Molecular Probes, 1:1000) for 48 h at 4°C.

Brain slices were fixed to a coverslip and then to a Petri dish using thin films of 5% agarose. Slices were viewed with a ×20/1 NA water-immersion objective mounted on an

© 2010 The Authors. Journal compilation © 2010 The Physiological Society

Table 1. The primers used for Qrt -PCR

Primers	Forward	Reverse
Kv1.1	GCA ACT GAT CAA AAC TGC GTT A	ATT GCT TGC CTG GTG CTT T
Kv1.2	TGC AAG GGC AAC GTC ACA	GGT CTG AAG CCT TTG GAA GGA
Kv3.1	CTT ATC AAC CGG GGA GTA CG	AAT GAC AGG GCT TTC TTT GC
Kv3.3	AGC TTG CTT CCT TGT CAC AGA CT	GCG GGA CTT CTC GTA ACC TTT
c-*fos*	CAA GCG GTA GGT TGA ACC AG	CCA TAG TCC CAA CCT CCA AC
β-Actin	CCC GCG AGT ACA ACC TTC T	CGT CAT CCA TGG CGA ACT

Axioskop 2FS (Carl Zeiss) and imaged using multi-photon excitation from a near IR pulsing laser tuned to 780 nm (Mai Tai DeepSee-Spectra Physics, Mountain View, CA, USA). Emissions were monitored at 560–615 nm for dextran and 500–550 nm for Kv3.1b (Alexa-fluor 488). Z-series images were collected with an optical section of 1.64 μm, and summed projections of labelled MNTB neurons were obtained.

Calcium imaging

Cultured slices, containing dextran retrograde labelled MNTB neurons, were loaded with 5 μM Fura-2 AM (Molecular Probes, Eugene, OR, USA, dissolved in dimethyl sulphoxide (DMSO) containing 5% pluronic acid) for 10 min in aCSF. Before recording, slices were kept in aCSF for 30 min to allow de-esterification of the AM dye, using techniques described previously (Billups *et al.* 2002). In order to avoid glial cell debris and dead neurons, fura-2 fluorescence (excitation at 340 and 380 nm) was recorded only in confirmed MNTB neurons containing the retrograde dextran signal (543 nm excitation wavelength). Before imaging, acute brain slices were incubated in normal aCSF containing 2 mM $[Ca^{2+}]_o$ for more than 1 h, allowing equilibrium of intracellular calcium. This imaging was conducted using an intensified CCD camera (PentaMax, Princeton Instruments, Inc.). The Fura-2 fluorescent image (emission > 505 nm) was displayed using MetaFluor imaging software (Series 7, Molecular Devices). The light source was a Polychrome II Monochromator (TILL Photonics, Martinsried, Germany). These experiments were performed at 37°C.

Basal calcium concentrations were measured and calculated using a standard equation for ratiometric dyes (Grynkiewicz *et al.* 1985):

$$[Ca^{2+}] = K_d \times (R - R_{min})/(R - R_{max}) \times S_{f2}/S_{b2}$$

where R is the background-corrected fluorescence ratio F_{340}/F_{380}, R_{max} and R_{min} are the fluorescence ratios of MNTB neurons under Ca^{2+}-free and Ca^{2+}-saturating conditions, respectively and $S_{f2}/S_{b2} = F_{380,\ \text{zero Ca}}/F_{380,\ \text{saturating Ca}}$. For the dissociation constant (K_d) of Fura-2, a value of 224 nM was appropriate for these experimental conditions (temperature = 37°C).

To assess the scope of $[Ca^{2+}]_i$ increases and effects of inhibitors, recordings were made during transition from 2.5 mM $[K^+]_o$ to either 5 mM or 25 mM for low and high $[K^+]_o$ cultures, respectively. Constant $[Cl^-]_o$ was maintained by NaCl substitution.

Quantitative real-time PCR (Qrt-PCR)

RNA extraction (each homogenate consisted of two MNTBs pooled from one organotypic slice) was carried out using two different methods. Total RNA was isolated using TRI-reagent (Sigma) and mRNA isolated using the QuickPick kit (Bio-Nobile) which uses oligo-dT coated magnetic particles to bind poly-A mRNA. RT-PCR was performed on 100 ng total RNA or whole reaction of mRNA with SuperScript III first strand synthesis kit (Invitrogen) using random hexamer primers. Similar results were given by the two methods, but the QuickPick method is more suitable for processing small amounts of tissue. The resulting cDNA was then used for fluorescence PCR (Power SYBR Green PCR Master Mix and ABI Prism 7000 thermal cycler; Applied Biosystems Inc., Foster City, CA, USA). Primers were design to cross exon–exon boundaries, and the concentrations were optimized (300–900 nM) to ensure that the efficiencies of the target amplification and the endogenous reference (β-actin) amplification were approximately equal. The sequences are shown in Table 1. Amplification occurred under the following conditions: 50°C 2 min, 95°C 10 min, followed by 95°C 15 s and 60°C 60 s for 40 cycles. Quantification was performed using the comparative C_T method ($\Delta\Delta C_T$) (User Bulletin 2, ABI Prism Sequence Detection System, pp. 11–15, 1997, PE Applied Biosystems). Each experiment was carried out on sister slices from the same animal raised in high $[K^+]_o$ with (treated) or without (control) treatment, and $\Delta\Delta C_T$ values of treated slices were normalized to their control slices.

Immunoblotting

MNTB regions were carefully dissected from sister organotypic slices of the same animal cultured in either 5 mM or 25 mM $[K^+]_o$ medium for 7 days. For each culture condition, either two slices were collected from one animal, or in later experiments four slices (from 2 animals) were combined. To extract protein, boiled

© 2010 The Authors. Journal compilation © 2010 The Physiological Society

loading buffer (Trizma-base pH 6.8 100 mM; glycerol 20%; SDS 4%; dithiothreitol 100 mM; and 0.2% bromophenol blue) was added to samples and boiled for 10 min (to block dephosphorylation and degradation of the proteins). Samples were then homogenized and centrifuged at 12 000 rpm for 3 min at room temperature. Equal volumes of supernatant from each sample were loaded twice onto a 10% SDS–polyacrylamide gel with a ladder of pre-stained proteins (10–250 kDa; Bio-Rad) loaded in between. After separation, proteins were transferred onto nitrocellulose membranes using a semi-dry transfer cell (30 min, 24 V; Bio-Rad). Membranes were blocked with 5% BSA in Tris-buffered saline (TBS: Tris-HCl pH 7.5 20 mM and NaCl 150 mM) overnight at 4°C. For blotting, the two identical columns from each sample were divided and probed with either rabbit anti-CREB 1:1000 or rabbit anti-phospho-CREB (Ser133) 1:500 (Cell Signaling Technology, Beverly, MA, USA) in TBS containing 5% BSA at 4°C for 8 h. Loading controls were performed by labelling the two columns of each sample with α-tubulin (1:5000, Sigma-Aldrich, UK). Signals were detected with an anti-rabbit IgG conjugated to horseradish peroxidase using enhanced chemiluminescence detection (GE Healthcare, Little Chalfont, UK). Results were quantified using densitometry and Image Quant 5.2 (Nonlinear Dynamics Ltd, Garth Heads, UK) software.

Statistics

Data were presented as the mean ± S.E.M. and analysed using Student's *t* test (paired or unpaired as indicated). A P value of < 0.05 was considered statistically significant.

Results

Organotypic cultures of brainstem slices from P9 to P12 rats were raised either in low or high $[K^+]_o$ extracellular medium (5 and 25 mM KCl, respectively). Electrophysiological or imaging experiments were conducted on MNTB neurons which had been maintained for 7–28 DIV or from acute brain slices. The MNTB was identified by the preserved cytoarchitecture of the superior olivary complex (Fig. 1*A* and *B*), and single neurons displayed

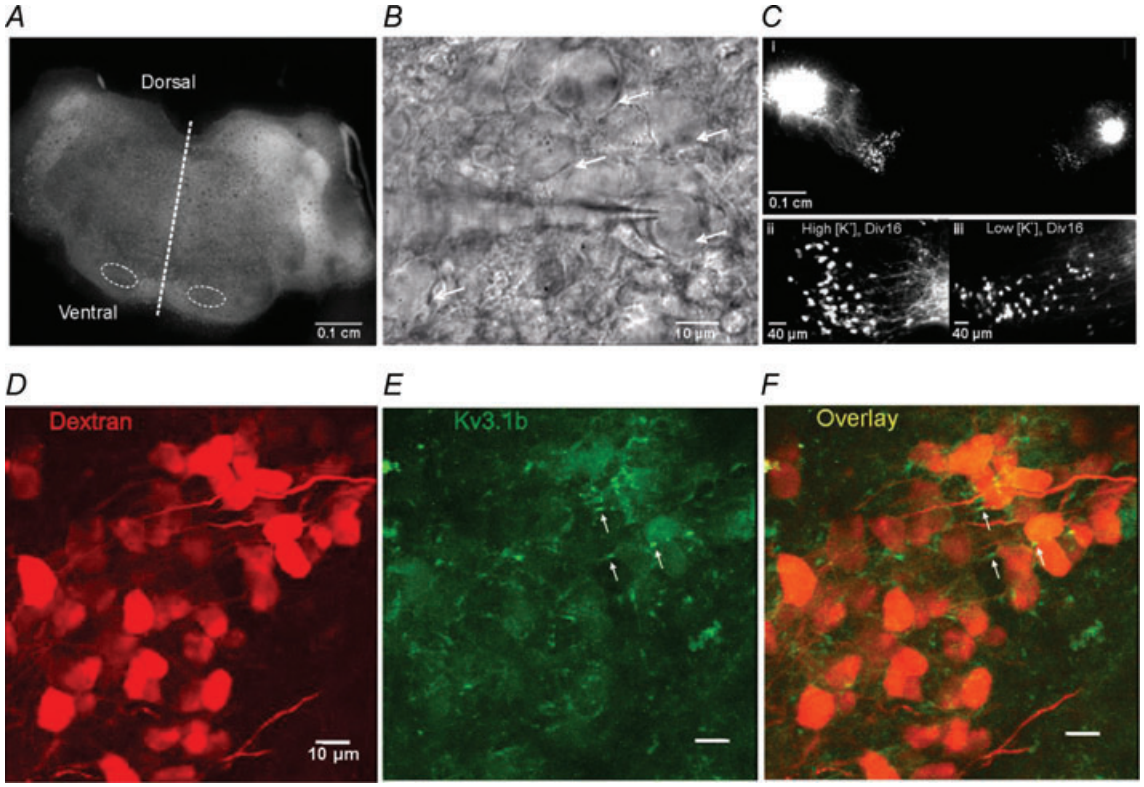

Figure 1. The MNTB maintains projections and neuronal morphology in organotypic culture
A, low magnification microphotograph showing preservation of a transverse brainstem slice after 10 DIV organotypic culture. Dashed line indicates midline; dashed circles indicate locations of the MNTBs. *B*, DIC image showing a patch pipette recording from an MNTB principle neuron (arrow) in an organotypic slice. *C*, unilateral dextran rhodamine (dextran) injection in LSO resulted in retrograde labelling in both MNTBs in an organotypic culture (*i*); higher magnification images show dextran labelled MNTB neurons in high $[K^+]_o$ (*ii*) and low $[K^+]_o$ (*iii*) cultures. *D–F*, confocal projection images of MNTB neurons showing co-labelling of dextran (red, *D*) with Kv3.1b (green, *E*). Cytoplasmic and putative initial segment region (arrow) staining of Kv3.1b was observed in the merged image (*F*).

© 2010 The Authors. Journal compilation © 2010 The Physiological Society

typical MNTB morphology (Forsythe, 1994). Both high and low $[K^+]_o$ culture media provided viable MNTB neurons from cultures prepared from P9 ($n = 5$), P10 ($n = 23$), P11 ($n = 29$) and P12 ($n = 5$), as confirmed by electroporation of fluorescent dextran in the LSO and retrograde axonal transport into the MNTB (Fig. 1*Cii* and *iii*). Fluorescence labelling evidence showed that the calyx of Held synapse was not maintained in long-term culture (online Supplemental Material, Supplementary Fig. S1). Nevertheless, subthreshold synaptic events were observed, consistent with spontaneous non-calyceal inputs. MNTB neurons raised in either low or high $[K^+]_o$ experienced a similar low frequency of the subthreshold events when exposed to 5 mM or 25 mM $[K^+]_o$ containing aCSF, respectively (low $[K^+]_o$, 0.009 ± 0.004 Hz $n = 6$; high $[K^+]_o$, 0.007 ± 0.004 Hz $n = 6$). Co-labelling of fluorescent dextran-labelled neurons with Kv3.1b antibody showed a similar expression pattern of Kv3.1b to acute brain slices (Dodson *et al.* 2003) with staining in the soma and proximal region of axons (probable initial segment; Fig. 1*D–F*).

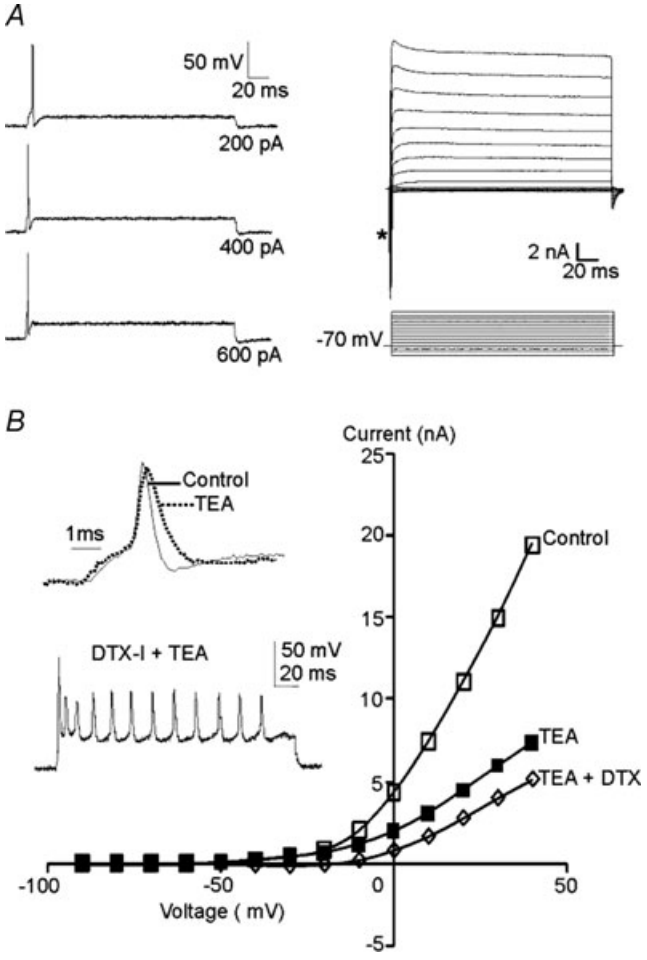

Figure 2. MNTB neurons cultured in high $[K^+]_o$ (25 mM) medium maintain their phenotypic single AP firing pattern and outward K^+ currents

A, left, current-clamp recording shows single fast APs are evoked in response to sustained depolarizing current injection (current magnitude indicated to the right of each trace). Resting membrane potential was adjusted to −70 mV. Right, voltage-clamp shows fast inward sodium currents (*) and sustained outward K^+ currents evoked by voltage step commands (10 mV increments; voltage traces below). *B*, current–voltage (*I–V*) relationships plotted for control (open squares), in the presence of 1 mM TEA (filled squares) and in the presence of both TEA and 100 nM dendrotoxin-I (DTX-I, open diamond). Insets show that TEA broadened the action potential (normalized to the same amplitude) and DTX-I induced multiple action potential firing.

Cultures in high $[K^+]_o$ medium exhibit greater K^+ currents

MNTB neurons raised in either low or high $[K^+]_o$ medium were compared to examine if the most basic neuronal stimulus, depolarization, influenced the intrinsic properties of MNTB neurons.

Under current clamp, MNTB neurons from high-K cultures responded to depolarizing current injection with a phenotypic single brief AP ($n = 10$; Fig. 2*A*, left) and sustained outward K^+ currents were evoked under voltage-clamp (following a rapid inward sodium current; Fig. 2*A*, right, *). MNTB neurons possess a TEA-sensitive high voltage-activated Kv3 K^+ conductance which contributes to rapid AP repolarization, and a dendrotoxin-I (DTX-I) sensitive low voltage-activated Kv1 conductance controlling AP threshold (Brew & Forsythe, 1995; Dodson *et al.* 2002). Kv1 conductances dominate at potentials between −40 and −30 mV, while Kv3 is additionally activated at voltages positive to around 0 mV (Brew & Forsythe, 1995; Dodson *et al.* 2002; Johnston *et al.* 2008). TEA (1 mM) reduced high voltage-activated K^+ currents, broadening the AP waveform (Fig. 2*B*) while DTX-I (100 nM) increased the number of evoked APs. These results are essentially identical to data from acute brain slices.

Comparison of the mean current–voltage (*I–V*) relations was conducted under identical conditions with aCSF containing $[K^+]_o$ of 2.5 mM and showed that in high-K cultures MNTB neurons ($n = 10$) were similar to those from acute brain slices ($n = 6$, Fig. 3*A*) while MNTB neurons raised in low $[K^+]_o$ ($n = 15$) exhibited smaller K^+ currents (−40 mV to +40 mV, $P < 0.05$). The low voltage-activated current (measured at −30 mV) was 0.6 ± 0.1 nA in low-K cultured neurons, compared to 1.3 ± 0.3 nA in high-K cultured and 1.7 ± 0.17 nA in acute brain slices. High voltage-activated currents (measured at +30 mV) were 11.3 ± 0.9 nA, 15.1 ± 1.8 nA and 17.5 ± 1.8 nA for low-K cultured, high-K and acute slices, respectively. The relative contributions of Kv3 and Kv1 conductance to the overall *I–V* relations are similar in the two culture conditions. TEA (1 mM) reduced the

© 2010 The Authors. Journal compilation © 2010 The Physiological Society

K^+ current measured at +30 mV by 51 ± 8% ($n = 5$) in low $[K^+]_o$ and 53 ± 8% ($n = 4$) in high $[K^+]_o$ cultures, while DTX-I (100 nM) blocked 59 ± 17% ($n = 4$) and 54 ± 11% ($n = 6$) of the currents measured at −30 mV for low and high-K cultures, respectively (Fig. 3*B*). Consistent with the *I–V* relations, current-clamp recordings revealed increased excitability in low-K cultures, although a single brief AP was always found at threshold (Fig. 3*C*). Multiple APs were fired for larger current injections ($n = 14$) with a lower AP threshold in low-K cultures (mean current at threshold: low-K: 156 ± 11 pA, $n = 16$; high-K: 225 ± 25 pA, $n = 10$, $P < 0.05$, Fig. 3*D*). The resting membrane potentials were −55 ± 1 mV ($n = 16$) for low-K cultures and −54 ± 1 mV ($n = 10$) for high-K cultures. Voltage-gated Na^+ currents at −40 mV were also lowest in low-K cultures (low-K: 9.6 ± 0.8 nA, $n = 15$; high-K: 12.5 ± 1.0 nA, $n = 9$, $P < 0.05$). The ratio of Na^+ and K^+ currents (at +40 mV) was similar in the two culture conditions (low-K, 0.81 ± 0.11, $n = 14$; high-K; 0.89 ± 0.07, $n = 9$, $P > 0.05$), supporting a similar AP waveform in the MNTB neurons. Together, these results show that organotypic cultures from animals over 1 week old and maintained in high $[K^+]_o$ culture medium had similar membrane properties to MNTB neurons in

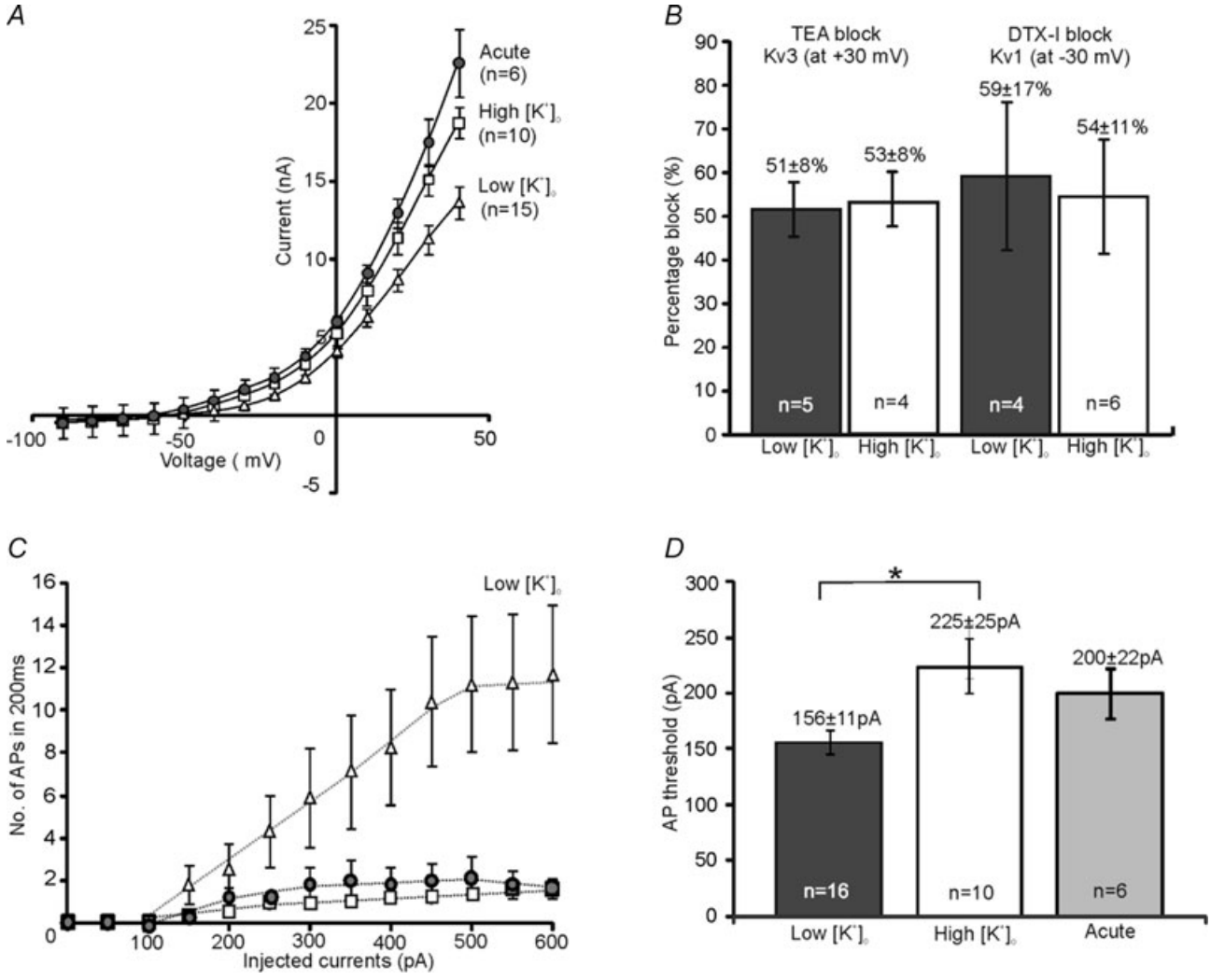

Figure 3. MNTB neurons cultured in low $[K^+]_o$ (5 mM) medium exhibit reduced K^+ currents and increased excitability

A, the mean *I–V* relations plotted for MNTB neurons from acute brain slices (filled circles), high-K cultures (open squares) and low-K cultures (open triangles). *B*, the percentage blocks of Kv3 (at +30 mV) and Kv1 (at −30 mV), induced by TEA (1 mM) and DTX-I (100 nM), respectively, are very similar in low (filled bars) and high-K (open bar) cultured neurons. *C*, a plot of the mean number of APs against the eliciting currents in current-clamp, acute brain slices (filled circles), high-K cultures (open squares) and low-K cultures (open triangles). *D*, MNTB neurons in low-K cultures (filled bar) exhibited significant (*) lower threshold to elicit APs when compared to neurons from high-K cultures (open bar) and acute brain slices (grey filled bar).

© 2010 The Authors. Journal compilation © 2010 The Physiological Society

acute brain slices, while low-K cultured neurons showed increased excitability due to lower K^+ current levels.

Calcium imaging revealed increased resting $[Ca^{2+}]_i$ in high $[K^+]_o$ cultures

It is often assumed that use of high K^+ medium provides a sustained depolarizing drive and continuous AP firing which mimics stimulation of excitatory synaptic inputs. However our direct current-clamp recordings show that AP firing was rapidly curtailed (Supplementary Fig. S2A), probably as a result of sodium channel inactivation (Ulbricht, 2005). This suggests that the $[K^+]_o$-induced changes in organotypic cultures are not due to increased AP firing or subsequent synaptic release, and suggests an alternative hypothesis where high $[K^+]_o$ causes depolarization-induced Ca^{2+} influx through VGCCs and/or Ca^{2+}-induced Ca^{2+} release (CICR) from intracellular stores. We asked if there is a difference in basal $[Ca^{2+}]_i$ during chronic depolarisation with $[K^+]_o$ concentrations above basal. And then we attempted to differentiate between Ca^{2+}-entry pathways, such as VGCCs and store-mediated Ca^{2+} release. $[Ca^{2+}]_i$ was measured by loading slices with the calcium-sensitive fluorescent dye Fura-2, and monitoring the fluorescence from identified MNTB neurons which were dextran-filled by retrograde labelling of dye injected into the LSO, as noted in the methods (Fig. 4*A* and *B*).

Basal $[Ca^{2+}]_i$ was compared between low and high-K cultures in 5 mM or 25 mM $[K^+]_o$ containing aCSF, respectively; we found that high-K cultures (73.3 ± 2.5 nM, $n = 21$, $P < 0.05$) have higher basal $[Ca^{2+}]_i$ compared to low-K cultures (41.6 ± 1.7 nM, $n = 40$). MNTB neurons in acute slices ($n = 20$) also had a higher $[Ca^{2+}]_i$ perhaps reflecting the recent slicing procedure (283.6 ± 8.0 nM).

The membrane potentials obtained under the different $[K^+]_o$ are shown in Supplementary Fig. S2; these depolarisations are across the range of voltages which would open VGCCs. We asked how $[K^+]_o$ depolarization affected $[Ca^{2+}]_i$ in the two culture conditions (low-K cultures (2.5 to 5 mM K^+) 6.4 ± 0.9 mV, $n = 8$; high-K cultures (2.5 to 25 mM K^+) 21.7 ± 2.2 mV, $n = 9$, Supplementary Fig. S2*B*). The high-K cultures exhibited greater acute increases in $[Ca^{2+}]_i$ (low-K cultures $35.5 \pm 2.0\%$, $n = 6$; high-K cultures $77.0 \pm 7.1\%$, $n = 18$, $P < 0.05$). The larger depolarisation could activate multiple Ca^{2+}-entry pathways, so the contribution of VGCCs or internal store release were tested. Bath application of a VGCC inhibitor cocktail (Nif, 10 μM, CTx-GVIA 2 μM and Aga-IVA 200 nM), prior to changes in $[K^+]_o$, reduced the relative $[Ca^{2+}]_i$ increase to $22.0 \pm 0.4\%$ in high-K cultured MNTB neurons ($n = 9$). Inhibition of intracellular store release by 100 μM Rya, a concentration that blocks ryanodine receptors (Buck *et al.* 1992; Verkhratsky, 2005), and 2-APB (100 μM, blocks IP_3 receptors) reduced the $[Ca^{2+}]_i$ increase in high-K cultures to $3.8 \pm 0.2\%$ ($n = 10$) (Fig. 4*D*). VGCCs played a prominent role, particularly in low-K cultures where VGCC blockers reduced $[Ca^{2+}]_i$ to $8.4 \pm 0.4\%$ ($n = 8$, $P < 0.05$, Supplementary Fig. S3), although Rya and 2-APB now had less impact ($21.1 \pm 0.8\%$, $n = 9$). Together these results suggest that the higher chronic $[Ca^{2+}]_i$ in MNTB neurons in high $[K^+]_o$ culture conditions may be involved in the longer-term changes in ion channel expression.

High $[K^+]_o$ induces further CREB phosphorylation during culture

Intracellular calcium is well established as a long-term mediator in transduction of synaptic activity into gene expression. Activity-dependent phosphorylation of the transcription factor CREB at Ser133 (p-CREB) is driven by cytosolic Ca^{2+} (Sheng *et al.* 1990; Brosenitsch & Katz, 2001; Deisseroth & Tsien, 2002; Kornhauser *et al.* 2002) and to test if global Ca^{2+} increase causes CREB phosphorylation in this organotypic preparation, we examined the ratio of p-CREB to CREB using Western blotting.

The high-K cultures enhanced the proportion of phosphorylated CREB over 7 days. The ratio of p-CREB to total CREB is 0.70 ± 0.15 in high-K cultures and 0.41 ± 0.15 in low-K cultures ($n = 3$, $P < 0.05$, Fig. 5). This result reveals another significant difference between the two culture conditions and is consistent with CREB-mediated gene expression underlying changes in intrinsic excitability.

Ca^{2+} store release and CREB are essential to maintain K^+ currents in high $[K^+]_o$ cultures

We next explored the functional impact of CICR and CREB activation on K^+ currents in high-K cultures. KG-501 is known to disrupt the association of CREB with a co-activator, the CREB binding protein (CBP) and attenuates CREB-mediated transcription (Best *et al.* 2004; Peltier *et al.* 2007). To allow sufficient time for changes in gene expression to be reflected in functional protein, high-K cultures were incubated with either CREB antagonist (KG-501, 12.5 μM) or intracellular store blockers (2-APB, 100 μM and Rya, 100 μM) for 24 to 48 h. Whole-cell recordings were subsequently made in normal aCSF and compared to sister controls ($n = 4$).

We found that AP waveforms were broadened from 0.58 ± 0.04 ms (sister control, $n = 4$) to 0.90 ± 0.11 ms ($n = 5$, $P < 0.05$) by 2-APB and Rya, and to 1.10 ± 0.11 ms ($n = 6$, $P < 0.05$) by KG-501 (Fig. 6*A*). The high voltage-activated K^+ currents (on steps to +20 mV to +40 mV) were reduced significantly by Rya and 2-APB

© 2010 The Authors. Journal compilation © 2010 The Physiological Society

($n = 5$, $P < 0.05$), and the mean K^+ current was reduced by 40% at +30 mV (Fig. 6*B*). Incubation with KG-501 induced a potent reduction of the K^+ current (on steps to −10 mV to +40 mV; $n = 5$, $P < 0.05$, 58% at +30 mV, Fig. 6*B*). No significant difference was found in the AP firing threshold or the firing pattern in KG-501 or Rya and 2-APB treated cultures, consistent with unchanged low voltage-activated K^+ currents.

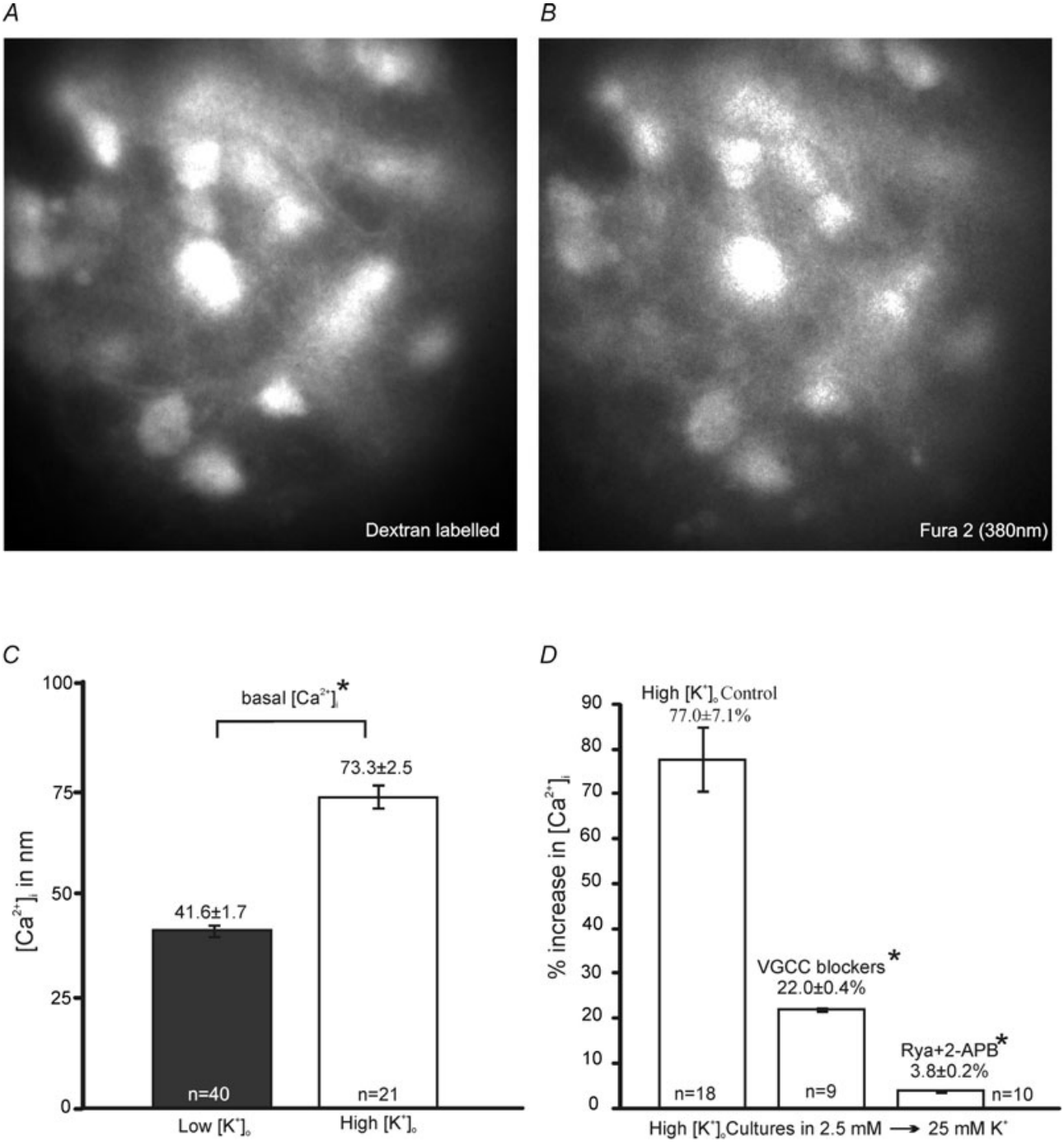

Figure 4. The rise in $[Ca^{2+}]_i$ in high-K cultures is mediated by VGCC influx and intracellular store release
A and *B*, representative fluorescence images of a group of MNTB neurons from organotypic slices with excitation wavelength at 543 nM for dextran tetramethyl-rhodamine (dextran) (*A*) and 380 nM for Fura2 labelling (*B*). *C*, high-K cultures (open bar) displayed significantly greater (*$P < 0.05$) basal $[Ca^{2+}]_i$ to low-K cultures (filled bar). *D*, summary of percentage increase of $[Ca^{2+}]_i$ in high-K cultures during changes of $[K^+]_o$ from 2.5 mM to 25 mM KCl containing aCSF. Perfusion of VGCC blockers (Nif 10 μM; CTx 2 μM; Aga 200 nM) and inhibition of store release ($P < 0.05$) by Rya (100 μM) and 2-APB (100 μM) both greatly reduced the change in $[Ca^{2+}]_i$ (*$P < 0.05$).

© 2010 The Authors. Journal compilation © 2010 The Physiological Society

These results suggest that Ca^{2+} release from stores and activation of CREB are both essential to maintain elevated levels of high voltage-activated K^+ currents in MNTB neurons.

Voltage-gated calcium channel blockers reduce K^+ currents in high-K cultures

Ca^{2+} influx through VGCCs can also contribute to $[Ca^{2+}]_i$, as shown in many studies (Power & Sah, 2005; Yu *et al.* 2008). The long-term effect of VGCC blockers was evaluated by incubation of high-K cultures with L- N- and P/Q-type calcium channel blockers (Nif 10 μM, CTx-GVIA 2 μM and Aga-IVA 200 nM) for between 48 to 60 h. Whole-cell recordings were subsequently made in normal aCSF (containing 2.5 mM $[K^+]_o$). Results were compared between MNTB neurons raised in high-K with ($n = 7$) or without (control, $n = 6$) incubation with VGCC blockers.

After incubation with VGCC blockers, MNTB neurons fired trains of APs on depolarization instead of the characteristic single AP, and the AP firing threshold was reduced from 183 ± 17 pA (control: $n = 6$) to 135 ± 9 pA (treated: $n = 7$, $P < 0.05$, Fig. 7*A*). The number of APs generated by current injections of 600 pA increased from 1.3 ± 0.2 in control to 6.4 ± 3.1 in treated MNTB neurons as summarized in Fig. 7*C*. In addition, the AP waveform broadened with half-widths increasing from 0.49 ± 0.02 ms (control: $n = 6$) to 0.66 ± 0.03 ms (treated: $n = 7$; $P < 0.05$, Fig. 7*B*). The normalised mean *I–V* relationship for treated neurons also showed a predictable change with both high- and low-threshold K^+ currents being reduced substantially (Fig. 7*D*). After block of VGCCs, the average low-threshold currents (measured at -30 mV) were reduced by 71% (control: 1.7 ± 0.3 nA; treated 0.5 ± 0.2 nA), and the average high-threshold currents (measured at $+30$ mV) were reduced by 41% (control: 12.7 ± 1.4, $n = 6$; treated: 7.5 ± 0.7, $n = 6$). Chronic block of VGCCs mimics blocking release from intracellular stores, reducing the high voltage-activated K^+ currents. VGCCs are also important for maintaining Kv1-mediated currents in high-K cultures. Together, these results suggest that Kv1 and Kv3 are differentially regulated by different Ca^{2+} signals.

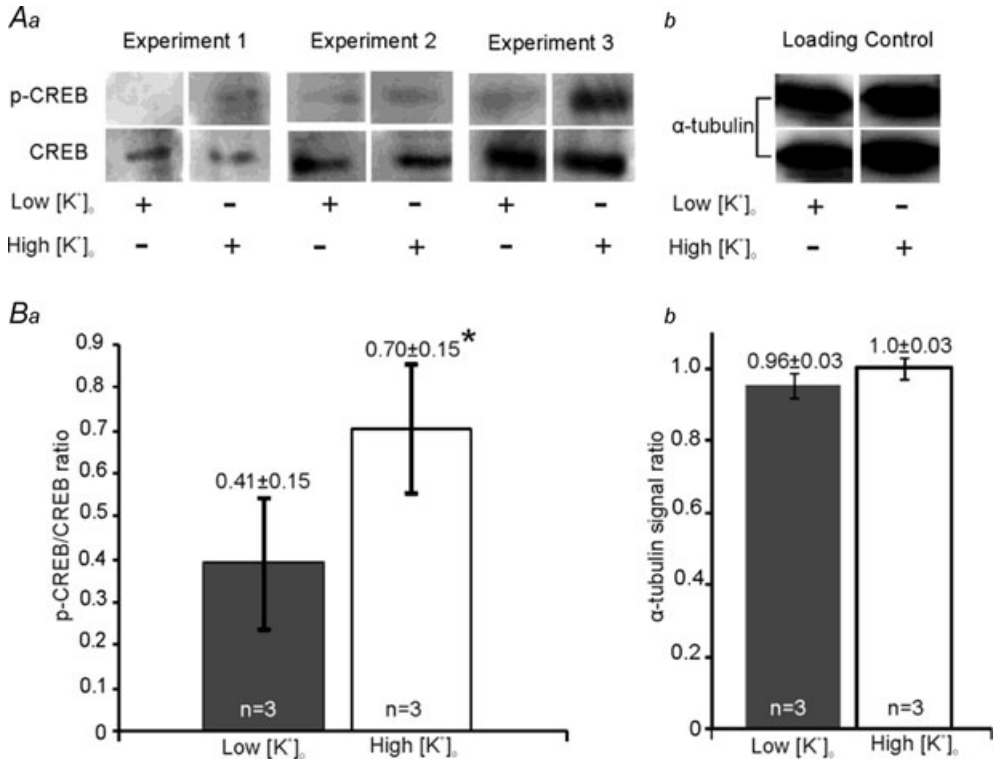

Figure 5. High $[K^+]_o$ cultures exhibited greater CREB phosphorylation
Aa, Western blots with the phosphorylated CREB (p-CREB) and total CREB (CREB) antibodies in low-K or high-K cultures from 3 individual experiments. *b*, representative loading control by α-tubulin shows equal protein loading of one sample onto two lanes labelled with p-CREB (above) and CREB (below). *Ba*, normalized ratio of phosphorylated CREB (p-CREB) to total CREB is significantly higher in high-K cultures (open bar) than in low-K cultures (filled bar). *b*, normalized α-tubulin signal ratio showed identical protein loading for lanes labelled with p-CREB and CREB antibody previously in both low (filled bar) and high-K cultures (open bar).

© 2010 The Authors. Journal compilation © 2010 The Physiological Society

CREB and VGCCs regulate Kv1.2, Kv.3.3 and c-*fos* expression in high $[K^+]_o$ cultures

High $[K^+]_o$ cultures exhibited elevated $[Ca^{2+}]_i$ and CREB function, which are essential for maintaining the K^+ currents, supporting the concept of activity-dependent Kv gene expression in the MNTB. Real-time PCR was performed to test the mRNA levels of Kv1.1, Kv1.2, Kv3.1 and Kv3.3. In addition, the immediate-early gene c-*fos* was examined, since it is targeted by CREB (Sheng & Greenberg, 1990; Sheng *et al.* 1990; Zhao *et al.* 2007) and is an established indicator for neuronal activity in the auditory brainstem (Luo *et al.* 1999; Miko *et al.* 2007).

High-K cultures showed higher mRNA levels of Kv1.1 (2.8 ± 0.2-fold, $n = 6$, $P < 0.05$) and Kv3.3 (4.1 ± 0.3-fold, $n = 6$, $P < 0.05$) relative to low-K cultures (Fig. 8*A*). Incubation with CREB antagonist (KG-501, 12.5 μM) for 48 h, reduced the mRNA expression of Kv3.3 to 0.6 ± 0.2-fold ($n = 9$, $P < 0.05$) and c-*fos* to 0.4 ± 0.2-fold ($n = 4$, $P < 0.05$, Fig. 8*B*), but potentiation of Kv1.1 mRNA levels was also observed (1.9 ± 0.1-fold, $n = 4$, $P < 0.05$) under these conditions. Blocking of VGCCs (Nif 10 μM; CTx-GVIA 2 μM and Aga-IVA 200 nM) produced similar results with reduced Kv3.3 mRNA (0.7 ± 0.2-fold, $n = 9$, $P < 0.05$) as well as c-*fos* (0.6 ± 0.3-fold, $n = 4$, $P < 0.05$) and increase in mRNA of Kv1.1 to 1.7 ± 0.5-fold ($n = 9$, $P < 0.05$). VGCC blockers also decreased Kv1.2 expression to 0.8 ± 0.3-fold ($n = 8$, $P < 0.05$, Fig. 8*C*). Although a cyclic AMP response element (CRE) for CREB binding has been shown on the rat Kv3.1 promoter (Gan *et al.* 1996), neither CREB antagonist nor VGCC blockers affected Kv3.1 mRNA significantly in this model.

Discussion

We have shown that MNTB neurons and their projections to the LSO are preserved in both low (5 mM) and high (25 mM) $[K^+]_o$ culture media when rat brainstem organotypic slices are prepared from P9–P12 animals. Neurons cultured in low $[K^+]_o$ medium exhibited increased excitability, while high $[K^+]_o$ cultures showed higher $[Ca^{2+}]_i$ and increased CREB phosphorylation and larger Kv currents. Block of calcium influx or block of Ca^{2+} release from intracellular stores decreased Kv3 currents, while block of VGCCs also reduced Kv1 channels. The CREB antagonist predominantly reduced Kv3-mediated current. These results show that activity-dependent changes in Kv currents are mediated by calcium signalling (via influx and release from intracellular stores) acting though a CREB signalling pathway, which may constitute a homeostatic mechanism, adjusting MNTB intrinsic excitability to depolarisation as a broad index of neuronal activity (Fig. 9).

Increased $[Ca^{2+}]_i$ rather than AP firing regulates MNTB excitability in high $[K^+]_o$

Several activity-dependent mechanisms affecting delayed rectifier K^+ channels have been reported previously, including, Kv2 phosphorylation in HEK cells (Park *et al.* 2006) and neurons (Misonou *et al.* 2006), Kv4 trafficking in hippocampal neurons (Kim *et al.* 2007) as well as

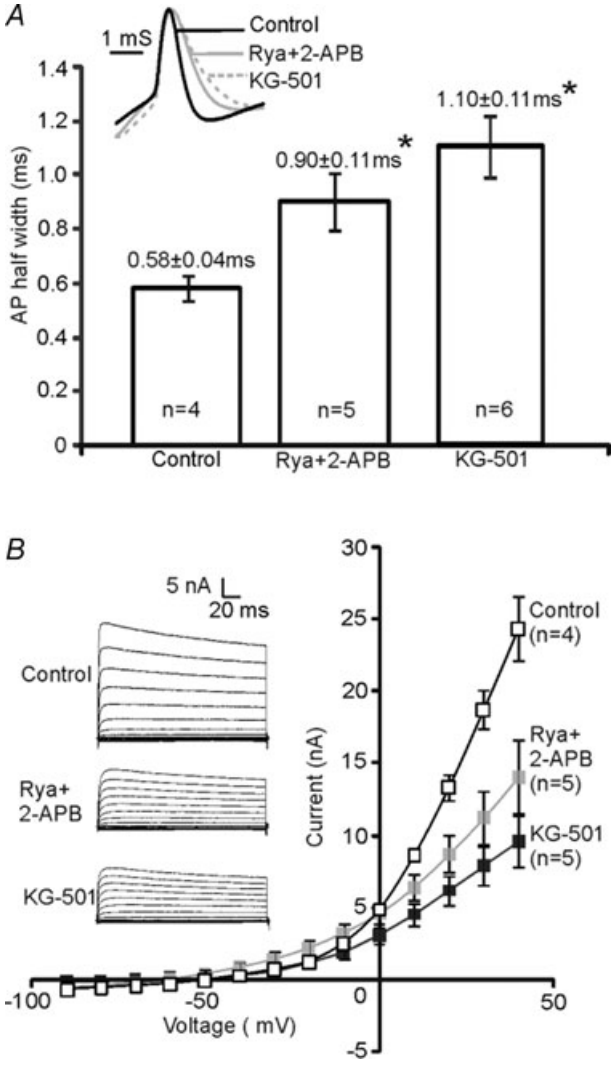

Figure 6. Inhibiting CREB or Ca^{2+} store release in high $[K^+]_o$ cultures reduced K^+ currents
A, the mean AP half-width increased from 0.58 ± 0.04 ms (control) to 0.90 ± 0.11 ms (Rya+2-APB treated) (*$P < 0.05$) and to 1.10 ± 0.11 ms (KG-501 treated) (*$P < 0.05$). Inset: superimposed AP waveforms (normalized to the same amplitude) illustrate broadening of APs with both treatments. *B*, the average *I–V* relationships show that Rya and 2-APB incubation reduced K^+ currents significantly between +20 and +40 mV ($P < 0.05$, grey filled squares), and KG-501 treated neurons (filled squares) exhibited less K^+ currents between −10 and +40 mV ($P < 0.05$, filled squares). Insets show a representative current trace for control, Rya+2-APB treated and KG-501 treated neurons; Na^+ current was truncated for better focus on K^+ currents.

© 2010 The Authors. Journal compilation © 2010 The Physiological Society

expression of Kv1 (Raab-Graham *et al.* 2006) and Kv3 channels (Liu & Kaczmarek, 1998) in hippocampus and inferior colliculus, respectively. Intrinsic membrane excitability is also regulated by other activity-dependent mechanisms (Desai *et al.* 1999; Nelson *et al.* 2003; Fan *et al.* 2005; Leao *et al.* 2005), and K^+-induced depolarization is often used to increase neuronal activity (Brosenitsch & Katz, 2001; Fan *et al.* 2005). In our study, high $[K^+]_o$ culture medium permitted maintenance of the MNTB single AP phenotype, while low $[K^+]_o$ medium increased excitability and AP firing and reduced K^+ currents. We first postulated that elevated K^+ caused depolarization-induced APs which triggered a homeostatic mechanism (by up-regulating potassium channels to control excitability). Counter-intuitively, high $[K^+]_o$ caused only transient elevation of AP firing, so chronic activity-dependent signalling must occur by other mechanisms. Independently of AP generation, depolarization evokes Ca^{2+} influx through VGCCs (Sheng *et al.* 1990; Berridge, 1998; West *et al.* 2001), and

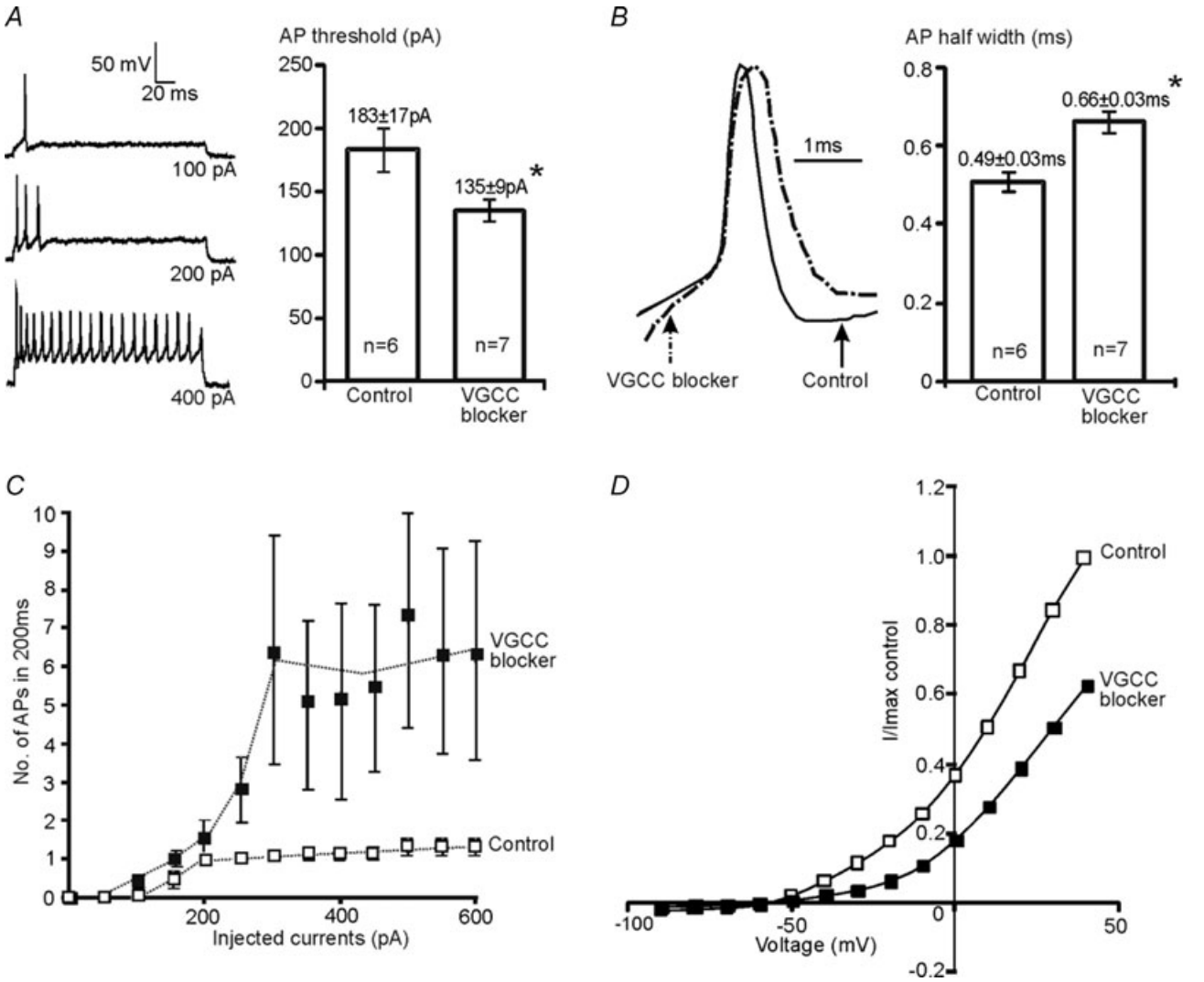

Figure 7. Chronic exposure to VGCC inhibitors attenuated K^+ currents in high $[K^+]_o$ cultures
A, representative responses to depolarizing current steps showed that MNTB neurons raised in high-K (left) failed to maintained the single AP phenotype after incubation with VGCC blockers Nif (nifedipine 10 μM), CTx (ω-conotoxin GVIA 2 μM) and Aga (ω-agatoxin IVA 200 nM). The neuron fired a single AP at a previous subthreshold stimulus (100 pA) followed by multiple APs generated at larger stimuli. Right, the mean AP firing threshold was significantly smaller in treated neurons ($^*P < 0.05$). *B*, representative traces show the AP waveform was broadened (left) after chronic block of Ca^{2+} influx through VGCCs. The mean AP half-width increased from 0.49 ± 0.02 ms (control) to 0.66 ± 0.03 ms (treated) ($^*P < 0.05$). *C*, the mean number of APs plotted against the eliciting currents, showes increased excitability in VGCC blocker treated neurons. *D*, the average *I–V* relationship (normalized to the maximum current in control neurons) showes that incubation with VGCC blockers (filled squares) substantially reduced outward K^+ currents.

© 2010 The Authors. Journal compilation © 2010 The Physiological Society

consequently promotes store filling (Rae *et al.* 2000; Power & Sah, 2005) or triggers store release (Jacobs & Meyer, 1997; Berridge, 1998; Meyer-Luehmann *et al.* 2002; Yu *et al.* 2008). A depolarization-induced reduction in intrinsic excitability mediated by L-type Ca^{2+} channels has recently been observed in primary hippocampal cultures (O'leary *et al.* 2010). Elevated intracellular Ca^{2+} forms a versatile mechanism of regulating excitability; for instance in hippocampal neurons, Ca^{2+} influx reduced excitability by up-regulating hyperpolarization-activated I_h channel expression (Fan *et al.* 2005) and in vestibular nucleus neurons, Nelson *et al.* (2003) suggest that transient reduction in intracellular Ca^{2+} increases intrinsic excitability.

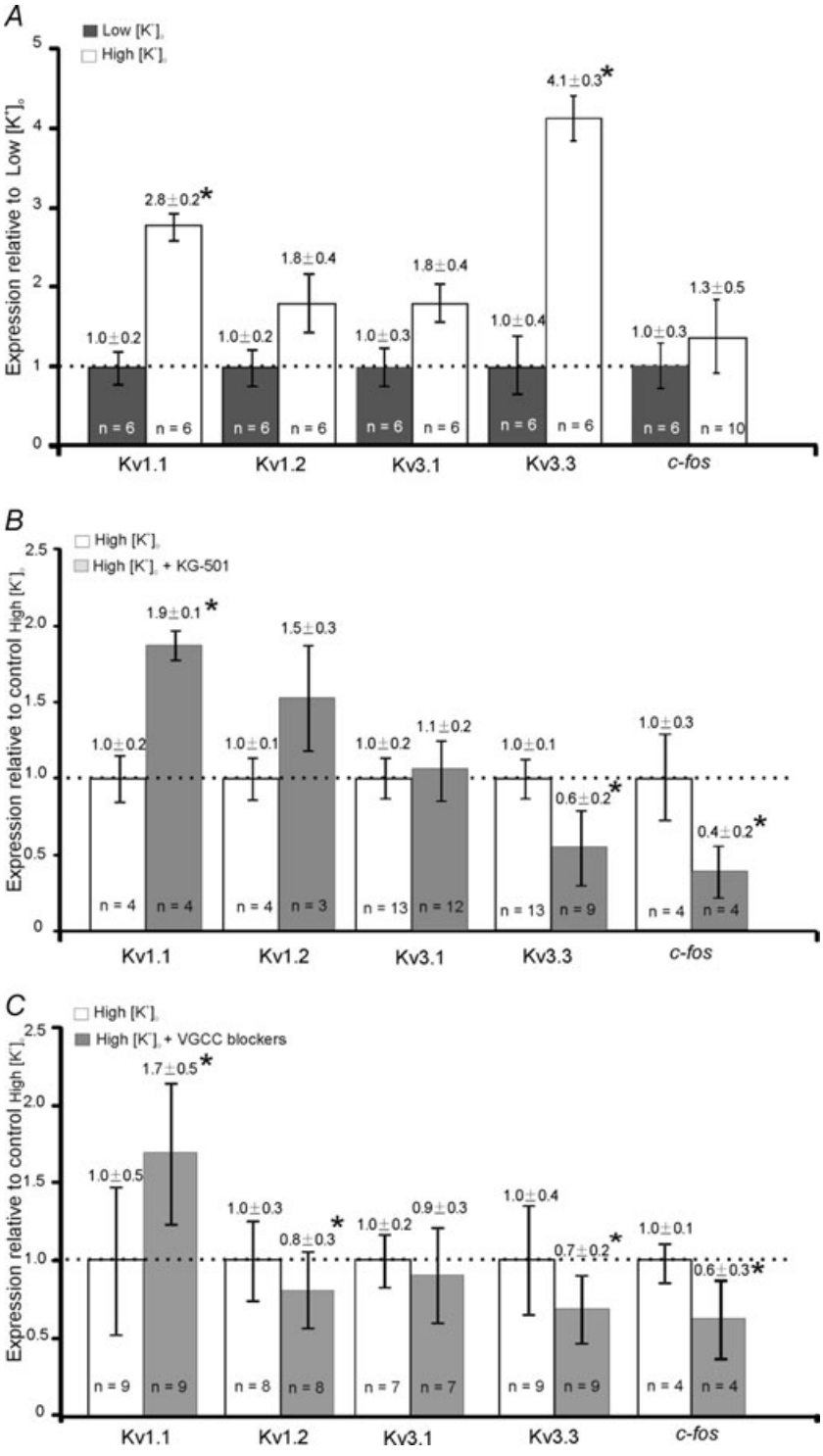

Figure 8. Comparison of K^+ channel mRNA expressed in cultures with low $[K^+]_o$, high $[K^+]_o$ and high $[K^+]_o$ incubated with either CREB antagonist or VGCC blockers
Expression of K^+ channel mRNA in the MNTB was estimated by Qrt-PCR. *A*, expression relative to low-K cultures; high-K cultures showed significantly ($^*P < 0.05$) higher levels of Kv1.1 and Kv3.3 mRNA expression. *B*, CREB antagonist (KG-501) reduced ($^*P < 0.05$) the mRNA levels of Kv3.3 and c-*fos* but potentiated Kv1.1 expression in high-K cultures. *C*, VGCC blockers (nifedipine, ω-conotoxin GVIA and ω-agatoxin IVA) reduced ($^*P < 0.05$) the mRNA levels of Kv1.2, 3.3 and c-*fos* but potentiated Kv1.1 expression in high-K cultures.

© 2010 The Authors. Journal compilation © 2010 The Physiological Society

Calcium imaging experiments revealed that MNTB neurons raised in high-K not only exhibit higher basal level of $[Ca^{2+}]_i$ but also experience increased $[Ca^{2+}]_i$ during depolarization, compared to low-K cultures. In high-K cultures, block of store release almost eliminated the $[Ca^{2+}]_i$ rise suggesting dominance of CICR; on the other hand VGCCs appeared to play a more dominant role in low-K cultures. Current-clamp recordings (Supplementary Fig. S2*B*) showed that 25 mM induced 21 ± 2 mV ($n = 9$) depolarization compared to 6 ± 1 mV ($n = 8$) in 5 mM $[K^+]_o$ relative to control 2.5 mM $[K^+]_o$. This difference mirrors the levels of plateau depolarization (supplementary Fig. S2*C*) achieved during sustained low frequency *versus* high frequency synaptic stimulation in the auditory system. That is, MNTB neurons experiencing high levels of spontaneous firing (average around 40 Hz) and/or peak sound-evoked firing rates *in vivo* (Kopp-Scheinpflug *et al.* 2003) are spending large periods of time depolarized to levels similar to that achieved on perfusion of 25 mM $[K^+]_o$. CICR has been shown to amplify AP induced Ca^{2+} influx depending on the number and frequency of the stimuli (Jacobs & Meyer, 1997). Together, this evidence suggests that the depolarization induced by 25 mM K^+ during culture would complement synaptically driven activities *in vivo* and consequently trigger CICR and tune excitability.

Elevated $[Ca^{2+}]_i$ triggers CREB-mediated up-regulation of K^+ channel expression

Optimal $[Ca^{2+}]_i$ is critical for cell survival and development in auditory neurons (Zirpel & Rubel, 1996; Zirpel *et al.* 1998) and as a second messenger, intracellular Ca^{2+} transforms neuronal activity into changes in gene expression through CREB, CaRF (the calcium-response factor) and NFAT (the nuclear factor of activated T-cells) (West *et al.* 2001, 2002). Among these transcription factors, CREB is closely coupled with Ca^{2+} elevation via VGCCs and ligand-gated ion channels (Brosenitsch & Katz, 2001; Hardingham *et al.* 2001; West *et al.* 2001; Zhao *et al.* 2007; Li *et al.* 2009).

Nuclear CREB phosphorylation at Ser133 is necessary to activate CREB-mediated transcription in neurons, and high $[K^+]_o$ cultures display significantly higher phosphorylated CREB. Reducing CREB activity by KG-501 functionally attenuated K^+ currents in the high voltage-activated Kv3 range (between −10 and +40 mV) in addition to down-regulating mRNA levels of Kv3.3, suggesting that CREB translates neuron activity into K^+ channel transcription. In the auditory pathway, Tan *et al.* (2008) showed an activity-dependent expression of p-CREB and brain-derived neurotrophic factor (BDNF) following chronic stimulation of cochlear implants in deaf

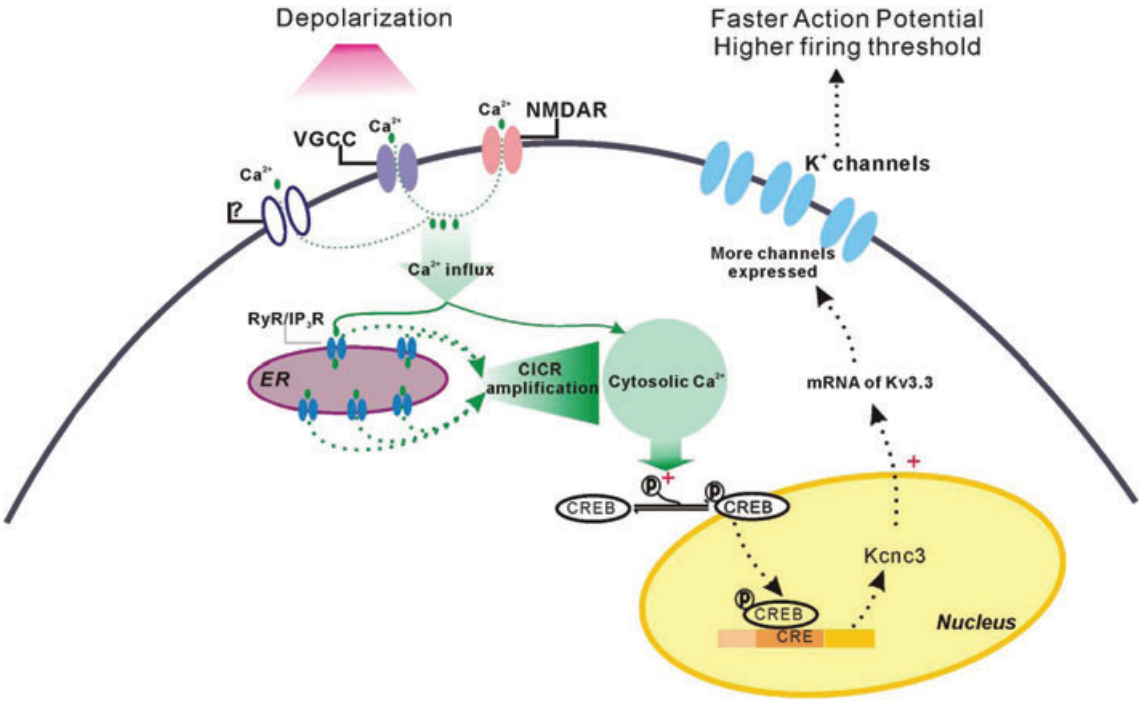

Figure 9. Depolarization-induced homeostatic regulation of K^+ channel expression
Upon depolarization, calcium influx through voltage-gated calcium channels (VGCCs) and ligand-gated channels (including NMDA receptors) elevates cytosolic Ca^{2+} and triggers ryanodine/ IP_3 sensitive Ca^{2+} release (CICR) from the endoplasmic reticulum (ER). The amplified Ca^{2+} signal promotes phosphorylation of CREB, which activates K^+ channel transcription, K^+ channel expression is up-regulated, and neurons become less excitable with faster action potentials and higher firing threshold.

© 2010 The Authors. Journal compilation © 2010 The Physiological Society

animals, consistent with the induction of postsynaptic p-CREB observed here.

The endoplasmic reticulum (ER) can act as a Ca^{2+} sink, buffering as well as amplifying Ca^{2+} signals and CICR may provide access for transmitting calcium signals from the cell surface into the nucleus (Hardingham *et al.* 1997; Jacobs & Meyer, 1997; Usachev & Thayer, 1997; Berridge, 1998; Power & Sah, 2005). Nevertheless, little is known about the link between CREB and IP_3/ryanodine receptor mediated store release (Ginsburg & Kimmel, 1989; Finkbeiner & Greenberg, 1998). Since calcium imaging experiments showed CICR regulated $[Ca^{2+}]_i$ in high-K cultures and blocked store release reduced Kv3 currents, it seems likely that CICR may mediate the CREB-dependent transcription. The Qrt-PCR results revealed that block of VGCCs induced a similar reduction of Kv3.3 and c-*fos* to those evoked by blocking CREB activity.

Versatile regulation of Kv expression by CREB and intracellular Ca^{2+}

Kv3.1 contains a CRE element located in its promoter (Gan *et al.* 1996; Kaczmarek *et al.* 2005), and von Hehn *et al.* (2004) showed that Kv3.1 tonotopicity accompanied p-CREB clustering in the MNTB. No significant difference in Kv3.1 expression was observed between the two culture conditions, and block of CREB function or VGCCs fails to affect Kv3.1 mRNA. However this may simply reflect that Kv3.3 message is more limiting of Kv3 channel production than Kv3.1 mRNA under these conditions. Kv1.1 message is higher in high-K cultures, but blocking either CREB or VGCC-mediated Ca^{2+} influx increased Kv1.1 expression in high-K cultures. Links between CREB signalling and Kv1 channels are suggested by over-expression of CREB in the nucleus accumbens shell (Wallace *et al.* 2009) which down-regulated Kv1.1 expression in socially isolated rats, but other activity-dependent mechanisms will also have an important role; for example, Raab-Graham *et al.* (2006) suggested an mTOR-dependent pathway in regulating Kv1.1 channel mRNA translation. Cytoplasmic Ca^{2+} regulates various kinase cascades and specifically regulates CREB function through multiple phosphorylation events (West *et al.* 2001; Deisseroth & Tsien, 2002; Kornhauser *et al.* 2002; West *et al.* 2002). Influx through NMDA receptors leads to transient phosphorylation of CREB through the calmodulin/CaM kinases IV-mediated pathway (Deisseroth *et al.* 1998; Ho *et al.* 2000; Kang *et al.* 2001), and Ca^{2+} influx through L-type Ca^{2+} channels triggers sustained phosphorylation through mitogen-activated protein kinase (MAPK) pathways (Dolmetsch *et al.* 2001; Wu *et al.* 2001). Brosenitsch & Katz (2001) showed that patterned stimulation activated N-type Ca^{2+} channel-mediated gene induction through a PKA and PKC involved pathway, while K^+-induced depolarization induced L-type Ca^{2+} channel-dependent expression through MAPK. Therefore, Ca^{2+} influx through VGCCs may integrate with CICR depending on calcium levels and/or channel subtype. In our study, the CREB mediated signalling selectively targeted Kv3.3 expression and function, but the results also suggested different regulatory pathways acting on Kv1 channels and further study is required to identify them.

Conclusion

Our experiments demonstrate that depolarization of MNTB neurons causes changes in functional expression of voltage-gated potassium channels in the membrane. This signalling pathway is mediated though increased $[Ca^{2+}]_i$ involving CICR, and activating CREB-dependent gene transcription, rather than APs or neurotransmitter release. We conclude that a Ca^{2+} and CREB-mediated homeostatic mechanism associated with membrane depolarisation regulates intrinsic excitability of MNTB neurons but does not require specific synaptic stimulation or AP firing.

References

Barnes-Davies M & Forsythe ID (1995). Pre- and postsynaptic glutamate receptors at a giant excitatory synapse in rat auditory brainstem slices. *J Physiol* **488**, 387–406.

Baxter AW & Wyllie DJ (2006). Phosphatidylinositol 3 kinase activation and AMPA receptor subunit trafficking underlie the potentiation of miniature EPSC amplitudes triggered by the activation of L-type calcium channels. *J Neurosci* **26**, 5456–5469.

Berridge MJ (1998). Neuronal calcium signalling. *Neuron* **21**, 13–26.

Best JL, Amezcua CA, Mayr B, Flechner L, Murawsky CM, Emerson B, Zor T, Gardner KH & Montminy M (2004). Identification of small-molecule antagonists that inhibit an activator: coactivator interaction. *Proc Natl Acad Sci U S A* **101**, 17622–17627.

Brew HM & Forsythe ID (1995). Two voltage-dependent K^+ conductances with complementary functions in postsynaptic integration at a central auditory synapse. *J Neurosci* **15**, 8011–8022.

Billups B, Wong AY & Forsythe ID (2002). Detecting synaptic connections in the medial nucleus of the trapezoid body using calcium imaging. *Pflugers Arch* **444**, 663–669.

Brosenitsch TA & Katz DM (2001). Physiological patterns of electrical stimulation can induce neuronal gene expression by activating N-type calcium channels. *J Neurosci* **21**, 2571–2579.

Buck E, Zimanyi I, Abramson JJ & Pessah IN (1992). Ryanodine stabilizes multiple conformational states of the skeletal muscle calcium release channel. *J Biol Chem* **267**, 23560–23567.

© 2010 The Authors. Journal compilation © 2010 The Physiological Society

Burger RM, Cramer KS, Pfeiffer JD & Rubel EW (2005). Avian superior olivary nucleus provides divergent inhibitory input to parallel auditory pathways. *J Comp Neurol* **481**, 6–18.

Chabbert C, Mechaly I, Sieso V, Giraud P, Brugeaud A, Lehouelleur J, Couraud F, Valmier J & Sans A (2003). Voltage-gated Na^+ channel activation induces both action potentials in utricular hair cells and brain-derived neurotrophic factor release in the rat utricle during a restricted period of development. *J Physiol* **553**, 113–123.

Chen Y, Stevens B, Chang J, Milbrandt J, Barres BA & Hell JW (2008). NS21: re-defined and modified supplement B27 for neuronal cultures. *J Neurosci Methods* **171**, 239–247.

Deisseroth K, Heist EK & Tsien RW (1998). Translocation of calmodulin to the nucleus supports CREB phosphorylation in hippocampal neurons. *Nature* **392**, 198–202.

Deisseroth K & Tsien RW (2002). Dynamic multiphosphorylation passwords for activity-dependent gene expression. *Neuron* **34**, 179–182.

Desai NS, Rutherford LC & Turrigiano GG (1999). Plasticity in the intrinsic excitability of cortical pyramidal neurons. *Nat Neurosci* **2**, 515–520.

Dodson PD, Barker MC & Forsythe ID (2002). Two heteromeric Kv1 potassium channels differentially regulate action potential firing. *J Neurosci* **22**, 6953–6961.

Dodson PD, Billups B, Rusznak Z, Szucs G, Barker MC & Forsythe ID (2003). Presynaptic rat Kv1.2 channels suppress synaptic terminal hyperexcitability following action potential invasion. *J Physiol* **550**, 27–33.

Dolmetsch RE, Pajvani U, Fife K, Spotts JM & Greenberg ME (2001). Signalling to the nucleus by an L-type calcium channel-calmodulin complex through the MAP kinase pathway. *Science* **294**, 333–339.

Fan Y, Fricker D, Brager DH, Chen X, Lu HC, Chitwood RA & Johnston D (2005). Activity-dependent decrease of excitability in rat hippocampal neurons through increases in I_h. *Nat Neurosci* **8**, 1542–1551.

Finkbeiner S & Greenberg ME (1998). Ca^{2+} channel-regulated neuronal gene expression. *J Neurobiol* **37**, 171–189.

Forsythe ID (1994). Direct patch recording from identified presynaptic terminals mediating glutamatergic EPSCs in the rat CNS, *in vitro*. *J Physiol* **479**, 381–387.

Gan L, Perney TM & Kaczmarek LK (1996). Cloning and characterization of the promoter for a potassium channel expressed in high frequency firing neurons. *J Biol Chem* **271**, 5859–5865.

Gibson JR, Bartley AF & Huber KM (2006). Role for the subthreshold currents I_{Leak} and I_H in the homeostatic control of excitability in neocortical somatostatin-positive inhibitory neurons. *J Neurophysiol* **96**, 420–432.

Ginsburg G & Kimmel AR (1989). Inositol trisphosphate and diacylglycerol can differentially modulate gene expression in *Dictyostelium*. *Proc Natl Acad Sci U S A* **86**, 9332–9336.

Grynkiewicz G, Poenie M & Tsien RY (1985). A new generation of Ca^{2+} indicators with greatly improved fluorescence properties. *J Biol Chem* **260**, 3440–3450.

Hardingham GE, Arnold FJ & Bading H (2001). A calcium microdomain near NMDA receptors: on switch for ERK-dependent synapse-to-nucleus communication. *Nat Neurosci* **4**, 565–566.

Hardingham GE, Chawla S, Johnson CM & Bading H (1997). Distinct functions of nuclear and cytoplasmic calcium in the control of gene expression. *Nature* **385**, 260–265.

Harris JA & Rubel EW (2006). Afferent regulation of neuron number in the cochlear nucleus: cellular and molecular analyses of a critical period. *Hear Res* **216–217**, 127–137.

Ho N, Liauw JA, Blaeser F, Wei F, Hanissian S, Muglia LM, Wozniak DF, Nardi A, Arvin KL, Holtzman DM, Linden DJ, Zhuo M, Muglia LJ & Chatila TA (2000). Impaired synaptic plasticity and cAMP response element-binding protein activation in Ca^{2+}/calmodulin-dependent protein kinase type IV/Gr-deficient mice. *J Neurosci* **20**, 6459–6472.

Hsieh CY & Cramer KS (2006). Deafferentation induces novel axonal projections in the auditory brainstem after hearing onset. *J Comp Neurol* **497**, 589–599.

Jacobs JM & Meyer T (1997). Control of action potential-induced Ca^{2+} signalling in the soma of hippocampal neurons by Ca^{2+} release from intracellular stores. *J Neurosci* **17**, 4129–4135.

Johnson HA & Buonomano DV (2007). Development and plasticity of spontaneous activity and Up states in cortical organotypic slices. *J Neurosci* **27**, 5915–5925.

Johnston J, Griffin SJ, Baker C, Skrzypiec A, Chernova T & Forsythe ID (2008). Initial segment Kv2.2 channels mediate a slow delayed rectifier and maintain high frequency action potential firing in medial nucleus of the trapezoid body neurons. *J Physiol* **586**, 3493–3509.

Kaczmarek LK, Bhattacharjee A, Desai R, Gan L, Song P, von Hehn CA, Whim MD & Yang B (2005). Regulation of the timing of MNTB neurons by short-term and long-term modulation of potassium channels. *Hear Res* **206**, 133–145.

Kang H, Sun LD, Atkins CM, Soderling TR, Wilson MA & Tonegawa S (2001). An important role of neural activity-dependent CaMKIV signalling in the consolidation of long-term memory. *Cell* **106**, 771–783.

Kim J, Jung SC, Clemens AM, Petralia RS & Hoffman DA (2007). Regulation of dendritic excitability by activity-dependent trafficking of the A-type K^+ channel subunit Kv4.2 in hippocampal neurons. *Neuron* **54**, 933–947.

Kivell BM, McDonald FJ & Miller JH (2000). Serum-free culture of rat post-natal and fetal brainstem neurons. *Brain Res Dev Brain Res* **120**, 199–210.

Kopp-Scheinpflug C, Fuchs K, Lippe WR, Tempel BL & Rubsamen R (2003). Decreased temporal precision of auditory signalling in Kcna1-null mice: an electrophysiological study in vivo. *J Neurosci* **23**, 9199–9207.

Kornhauser JM, Cowan CW, Shaywitz AJ, Dolmetsch RE, Griffith EC, Hu LS, Haddad C, Xia Z & Greenberg ME (2002). CREB transcriptional activity in neurons is regulated by multiple, calcium-specific phosphorylation events. *Neuron* **34**, 221–233.

Leao RN, Berntson A, Forsythe ID & Walmsley B (2004). Reduced low-voltage activated K^+ conductances and enhanced central excitability in a congenitally deaf (*dn*/*dn*) mouse. *J Physiol* **559**, 25–33.

Leao RN, Svahn K, Berntson A & Walmsley B (2005). Hyperpolarization-activated (I) currents in auditory brainstem neurons of normal and congenitally deaf mice. *Eur J Neurosci* **22**, 147–157.

© 2010 The Authors. Journal compilation © 2010 The Physiological Society

Li S, Zhang C, Takemori H, Zhou Y & Xiong ZQ (2009). TORC1 regulates activity-dependent CREB-target gene transcription and dendritic growth of developing cortical neurons. *J Neurosci* **29**, 2334–2343.

Liu SQ & Kaczmarek LK (1998). Depolarization selectively increases the expression of the Kv3.1 potassium channel in developing inferior colliculus neurons. *J Neurosci* **18**, 8758–8769.

Lohmann C, Ilic V & Friauf E (1998). Development of a topographically organized auditory network in slice culture is calcium dependent. *J Neurobiol* **34**, 97–112.

Lohrke S, Kungel M & Friauf E (1998). Electrical membrane properties of trapezoid body neurons in the rat auditory brain stem are preserved in organotypic slice cultures. *J Neurobiol* **36**, 395–409.

Luo L, Ryan AF & Saint Marie RL (1999). Cochlear ablation alters acoustically induced c-fos mRNA expression in the adult rat auditory brainstem. *J Comp Neurol* **404**, 271–283.

Meyer-Luehmann M, Thompson JF, Berridge KC & Aldridge JW (2002). Substantia nigra pars reticulata neurons code initiation of a serial pattern: implications for natural action sequences and sequential disorders. *Eur J Neurosci* **16**, 1599–1608.

Miko IJ, Nakamura PA, Henkemeyer M & Cramer KS (2007). Auditory brainstem neural activation patterns are altered in EphA4- and ephrin-B2-deficient mice. *J Comp Neurol* **505**, 669–681.

Misonou H, Menegola M, Mohapatra DP, Guy LK, Park KS & Trimmer JS (2006). Bidirectional activity-dependent regulation of neuronal ion channel phosphorylation. *J Neurosci* **26**, 13505–13514.

Muller YL, Reitstetter R & Yool AJ (1998). Regulation of Ca^{2+}-dependent K^+ channel expression in rat cerebellum during postnatal development. *J Neurosci* **18**, 16–25.

Nelson AB, Krispel CM, Sekirnjak C & du Lac S (2003). Long-lasting increases in intrinsic excitability triggered by inhibition. *Neuron* **40**, 609–620.

O'Leary T, van Rossum MC & Wyllie DJ (2010). Homeostasis of intrinsic excitability in hippocampal neurones: dynamics and mechanism of the response to chronic depolarization. *J Physiol* **588**, 157–170.

Oliver DL, Beckius GE, Bishop DC, Loftus WC & Batra R (2003). Topography of interaural temporal disparity coding in projections of medial superior olive to inferior colliculus. *J Neurosci* **23**, 7438–7449.

Park KS, Mohapatra DP, Misonou H & Trimmer JS (2006). Graded regulation of the Kv2.1 potassium channel by variable phosphorylation. *Science* **313**, 976–979.

Peltier J, O'Neill A & Schaffer DV (2007). PI3K/Akt and CREB regulate adult neural hippocampal progenitor proliferation and differentiation. *Dev Neurobiol* **67**, 1348–1361.

Power JM & Sah P (2005). Intracellular calcium store filling by an L-type calcium current in the basolateral amygdala at subthreshold membrane potentials. *J Physiol* **562**, 439–453.

Raab-Graham KF, Haddick PC, Jan YN & Jan LY (2006). Activity- and mTOR-dependent suppression of Kv1.1 channel mRNA translation in dendrites. *Science* **314**, 144–148.

Rae MG, Martin DJ, Collingridge GL & Irving AJ (2000). Role of Ca^{2+} stores in metabotropic L-glutamate receptor-mediated supralinear Ca^{2+} signalling in rat hippocampal neurons. *J Neurosci* **20**, 8628–8636.

Rubel EW & Fritzsch B (2002). Auditory system development: primary auditory neurons and their targets. *Annu Rev Neurosci* **25**, 51–101.

Russell FA & Moore DR (1995). Afferent reorganisation within the superior olivary complex of the gerbil: development and induction by neonatal, unilateral cochlear removal. *J Comp Neurol* **352**, 607–625.

Schneggenburger R & Forsythe ID (2006). The calyx of Held. *Cell Tissue Res* **326**, 311–337.

Sheng M & Greenberg ME (1990). The regulation and function of c-fos and other immediate early genes in the nervous system. *Neuron* **4**, 477–485.

Sheng M, McFadden G & Greenberg ME (1990). Membrane depolarization and calcium induce c-fos transcription via phosphorylation of transcription factor CREB. *Neuron* **4**, 571–582.

Song P, Yang Y, Barnes-Davies M, Bhattacharjee A, Hamann M, Forsythe ID, Oliver DL & Kaczmarek LK (2005). Acoustic environment determines phosphorylation state of the Kv3.1 potassium channel in auditory neurons. *Nat Neurosci* **8**, 1335–1342.

Steinert J, Kopp-Scheinpflug C, Baker C, Challiss R, Mistry R, Haustein M, Griffin S, Tong H, Graham B & Forsythe I (2008). Nitric oxide is a volume transmitter regulating postsynaptic excitability at a glutamatergic synapse. *Neuron* **60**, 642–656.

Stone TW (1993). Neuropharmacology of quinolinic and kynurenic acids. *Pharmacol Rev* **45**, 309–379.

Stoppini L, Buchs PA & Muller D (1991). A simple method for organotypic cultures of nervous tissue. *J Neurosci Methods* **37**, 173–182.

Tan J, Widjaja S, Xu J & Shepherd RK (2008). Cochlear implants stimulate activity-dependent CREB pathway in the deaf auditory cortex: implications for molecular plasticity induced by neural prosthetic devices. *Cereb Cortex* **18**, 1799–1813.

Tierney TS, Russell FA & Moore DR (1997). Susceptibility of developing cochlear nucleus neurons to deafferentation-induced death abruptly ends just before the onset of hearing. *J Comp Neurol* **378**, 295–306.

Trune DR (1982). Influence of neonatal cochlear removal on the development of mouse cochlear nucleus: I. Number, size, and density of its neurons. *J Comp Neurol* **209**, 409–424.

Uesaka N, Hirai S, Maruyama T, Ruthazer ES & Yamamoto N (2005). Activity dependence of cortical axon branch formation: a morphological and electrophysiological study using organotypic slice cultures. *J Neurosci* **25**, 1–9.

Ulbricht W (2005). Sodium channel inactivation: molecular determinants and modulation. *Physiol Rev* **85**, 1271–1301.

Urenjak J & Obrenovitch TP (2000). Kynurenine 3-hydroxylase inhibition in rats: effects on extracellular kynurenic acid concentration and N-methyl-D-aspartate-induced depolarisation in the striatum. *J Neurochem* **75**, 2427–2433.

© 2010 The Authors. Journal compilation © 2010 The Physiological Society

Usachev YM & Thayer SA (1997). All-or-none Ca^{2+} release from intracellular stores triggered by Ca^{2+} influx through voltage-gated Ca^{2+} channels in rat sensory neurons. *J Neurosci* **17**, 7404–7414.

Verkhratsky A (2005). Physiology and pathophysiology of the calcium store in the endoplasmic reticulum of neurons. *Physiol Rev* **85**, 201–279.

von Hehn CA, Bhattacharjee A & Kaczmarek LK (2004). Loss of Kv3.1 tonotopicity and alterations in cAMP response element-binding protein signalling in central auditory neurons of hearing impaired mice. *J Neurosci* **24**, 1936–1940.

Wallace DL, Han MH, Graham DL, Green TA, Vialou V, Iniguez SD, Cao JL, Kirk A, Chakravarty S, Kumar A, Krishnan V, Neve RL, Cooper DC, Bolanos CA, Barrot M, McClung CA & Nestler EJ (2009). CREB regulation of nucleus accumbens excitability mediates social isolation-induced behavioural deficits. *Nat Neurosci* **12**, 200–209.

West AE, Chen WG, Dalva MB, Dolmetsch RE, Kornhauser JM, Shaywitz AJ, Takasu MA, Tao X & Greenberg ME (2001). Calcium regulation of neuronal gene expression. *Proc Natl Acad Sci U S A* **98**, 11024–11031.

West AE, Griffith EC & Greenberg ME (2002). Regulation of transcription factors by neuronal activity. *Nat Rev Neurosci* **3**, 921–931.

Wu GY, Deisseroth K & Tsien RW (2001). Activity-dependent CREB phosphorylation: convergence of a fast, sensitive calmodulin kinase pathway and a slow, less sensitive mitogen-activated protein kinase pathway. *Proc Natl Acad Sci U S A* **98**, 2808–2813.

Xu J, Kang N, Jiang L, Nedergaard M & Kang J (2005). Activity-dependent long-term potentiation of intrinsic excitability in hippocampal CA1 pyramidal neurons. *J Neurosci* **25**, 1750–1760.

Yu HM, Wen J, Wang R, Shen WH, Duan S & Yang HT (2008). Critical role of type 2 ryanodine receptor in mediating activity-dependent neurogenesis from embryonic stem cells. *Cell Calcium* **43**, 417–431.

Zhao R, Liu L & Rittenhouse AR (2007). Ca^{2+} influx through both L- and N-type Ca^{2+} channels increases c-fos expression by electrical stimulation of sympathetic neurons. *Eur J Neurosci* **25**, 1127–1135.

Zirpel L, Lippe WR & Rubel EW (1998). Activity-dependent regulation of $[Ca^{2+}]_i$ in avian cochlear nucleus neurons: roles of protein kinases A and C and relation to cell death. *J Neurophysiol* **79**, 2288–2302.

Zirpel L & Rubel EW (1996). Eighth nerve activity regulates intracellular calcium concentration of avian cochlear nucleus neurons via a metabotropic glutamate receptor. *J Neurophysiol* **76**, 4127–4139.

Author contributions

H.T. prepared cultures, conducted experiments, analysed data and wrote the MS drafts. J.R.S. conducted calcium imaging experiments and advised on experimental design. S.W.R. conducted and analysed PCR experiments. T.C. advised on and supervised Western blot experiments. D.R. conducted multiphoton imaging. D.L.O. advised on and participated in dextran labelling experiments. I.D.F. conceived the project, supervised and assisted the project, and worked closely with H.T. in designing experiments, interpreting data and constructing figures and writing the manuscript. All authors contributed to writing the MS and approved the final version for publication.

Acknowledgements

We would like to thank Elena Ziviani and Daniele Bano for advice on optimizing Western blot experiments. Many thanks to Conny Kopp-Scheinpflug for comments on the draft manuscript. We appreciate Karina S. Cramer's advice on electroporation of fluorescent dextran. This work was funded by the Medical Research Council.

© 2010 The Authors. Journal compilation © 2010 The Physiological Society